ArbiTER studies of filamentary structures in the SOL of spherical tokamaks

D. A. Baver, J. R. Myra, Lodestar Research Corporation

F. Scotti, Lawrence Livermore National Laboratory

S. J. Zweben, Princeton Plasma Physics Laboratory

F. Militello, N. Walkden, CCFE, Culham Science Center

ArbiTER studies of filamentary structures in the SOL of spherical tokamaks

D. A. Baver a), J. R. Myra a), F. Scotti,b) S.J. Zweben,c) F. Militello, d) N. Walkden d)
a) Lodestar Research Corporation, Boulder, CO
b) Lawrence Livermore National Laboratory, Livermore, CA
c) Princeton Plasma Physics Laboratory, Princeton, NJ
d) CCFE, Culham Science Centre, Abingdon, UK

Filamentary structures in the scrape-off layer (i.e. blobs and ELM's) are an important source of cross-field transport in tokamaks. These structures affect scrape-off layer width, divertor heat deposition profiles and interaction with the main chamber walls.

The ArbiTER code[1] is applied here to provide insight into these structures. By using a perturbed density profile, it is possible to apply a linear eigenvalue code to determine important characteristics of these filamentary structures. Of particular interest is the penetration of such structures to the divertor plate. This is important for assessing the effect of such structures on divertor plate damage and erosion as well as the turbulent coupling between the midplane SOL and divertor region.

These studies concentrate on cases relevant to the NSTX and MAST experiments. By using experimental magnetic reconstruction profiles from these experiments, one can determine the characteristics of these filamentary structures in spherical tokamak geometries. Calculations relevant to future comparison with experimental data will be presented.

1. D. A. Baver, J. R. Myra and M. V. Umansky, Comm. Comp. Phys. **20**, 136 (2016).

Work supported by the U.S. Department of Energy Office of Science, Office of Fusion Energy Sciences, under Award Number DE-FG02-02ER54678 and DE-AC52-07NA27344.

Outline

- Motivation
- Tools and techniques
- Equilibrium solver
- Test method
- Results
- Conclusions

Motivation

- Filamentary structures ("blobs" and ELMs) are produced by edge turbulence and propagate into the SOL.
- Radial penetration of filaments in the SOL, important for main chamber wall interactions, is governed by a competition between radial convection ($V_r \sim \gamma/k$) and parallel loss processes.
- Parallel penetration of filaments determines their interaction with the divertor plates – important for material damage and erosion.
- Linear growth rates and parallel mode structure provide insight into these processes and predictions for their dependence on plasma parameters.

Motivation

- Studies of filament mode structure may help answer open questions such as:
  - What is the physical mechanism leading to the quiescent x-point region (QXR)?
  - Are divertor leg filaments truly local, or related to upstream filaments?
  - How does correlation between divertor fluctuations and upstream filaments vary with plasma parameters?

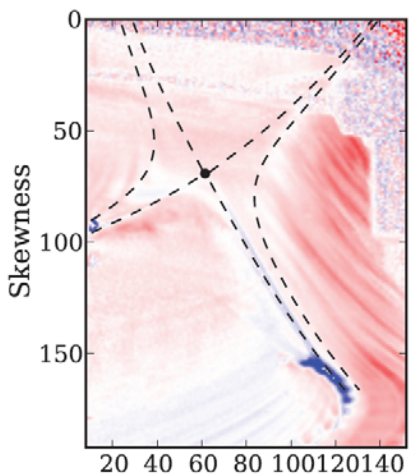

MAST raw Photron camera data
From: Walkden *et al,* 2017 meeting, showing skewness of fluctuations in the main SOL and a quiescent x-point region.

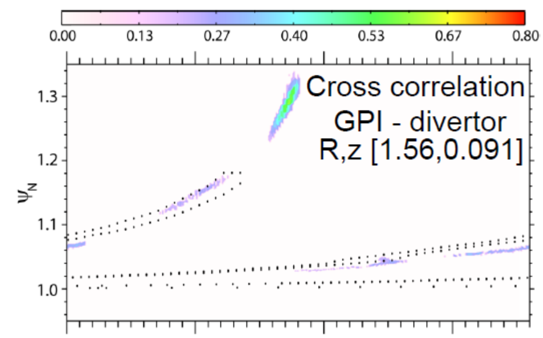

Midplane to divertor correlation near separatrix in NSTX (Scotti *et al,* 2017 meeting).

Tools and Techniques

- The Arbitrary Topology Equation Reader (ArbiTER) is a flexible code for solving linear PDE's in diverse geometries.
- PDE's are discretized using finite difference methods.
  - Recent upgrade also permits finite element methods.
- Model equations are defined using a specialized equation parser.
  - Inherited from the edge fluid eigenvalue code 2DX*.
- ArbiTER expands these capabilities by adding a topology parser.
  - Permits arbitrary connectivity.
  - Permits variable number of dimensions.
- Two main variants employed in this project:
  - Eigensolver (SLEPc based) used to calculate growth rates and mode structures of dominant instabilities.
  - Source-driven (PETSc based) used iteratively to calculate equilibrium temperature and density profiles.

Equilibrium solver

- Source driven code used to solve heat conduction equation:

$$\frac{1}{n_0}\,\partial_\perp n_0\,\chi_\perp\,\partial_\perp \tilde{T}_e + \partial_\parallel\,\chi_{\parallel 0}\,T_e^{5/2}\,\nabla_\parallel \tilde{T}_e = S$$

  – Source at inner radial boundary.
  – Perpendicular conductivity profile constructed artificially.
- Iterative method used to address nonlinear effects.
  – Parallel conductivity and boundary conditions calculated based on temperature and density profiles from previous iteration.
  – Density calculated by assuming minimum density fits some profile, then calculating pressure balance.
  – Parallel flows assumed to be localized near divertor.
    - Assumes high recycling regime.
- Density perturbation applied to final iteration.

Equilibrium solver

- Example solution at flux surface of interest:

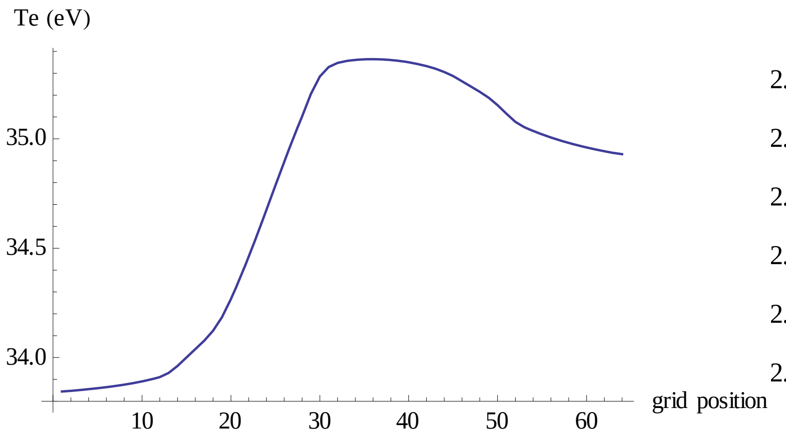

Temperature profile

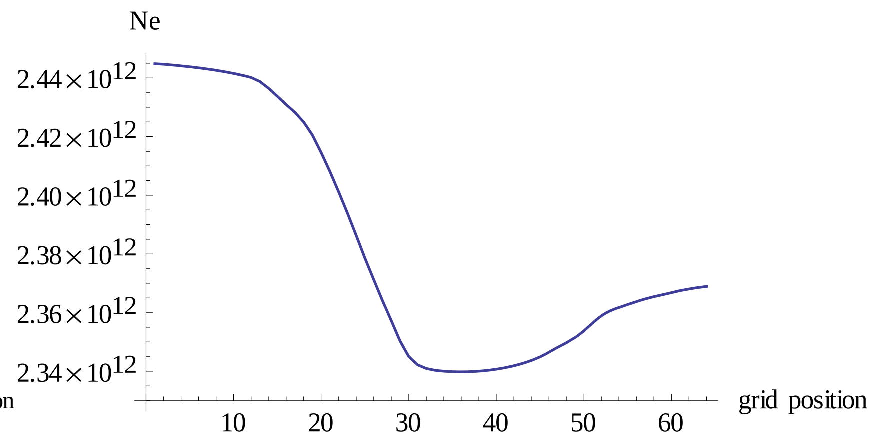

Density profile

Test method

- Resistive ballooning model is used.
- Magnetic geometry from EFIT reconstruction.
  – Data available from NSTX and MAST.
- Density and temperature profiles are artificially applied.
  – May be calculated using equilibrium solver or tanh-like profile may be used instead.
- Eigenmode localized at location of filamentary structure by applying density perturbation near specified flux surface.
- Ratio of amplitudes at various locations used to quantify mode penetration.

Test method

Base case density profile:

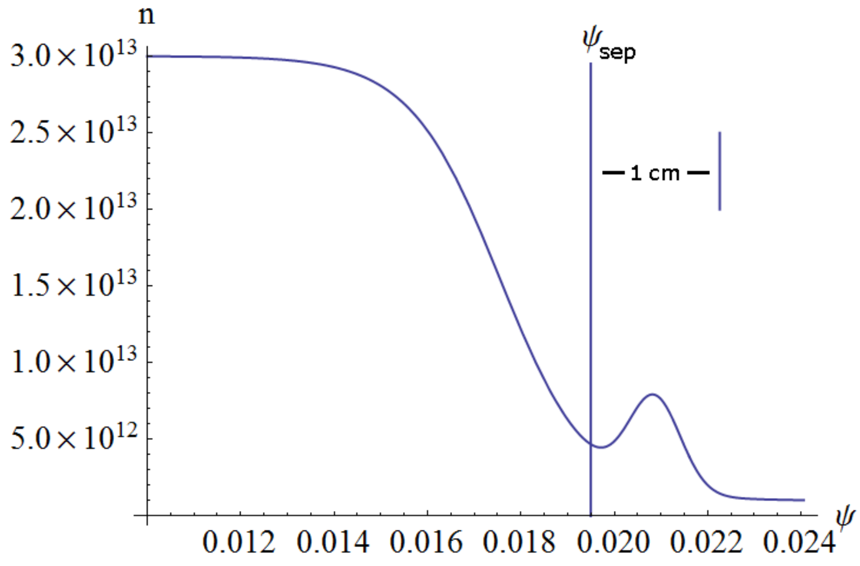

Base case temperature profile:

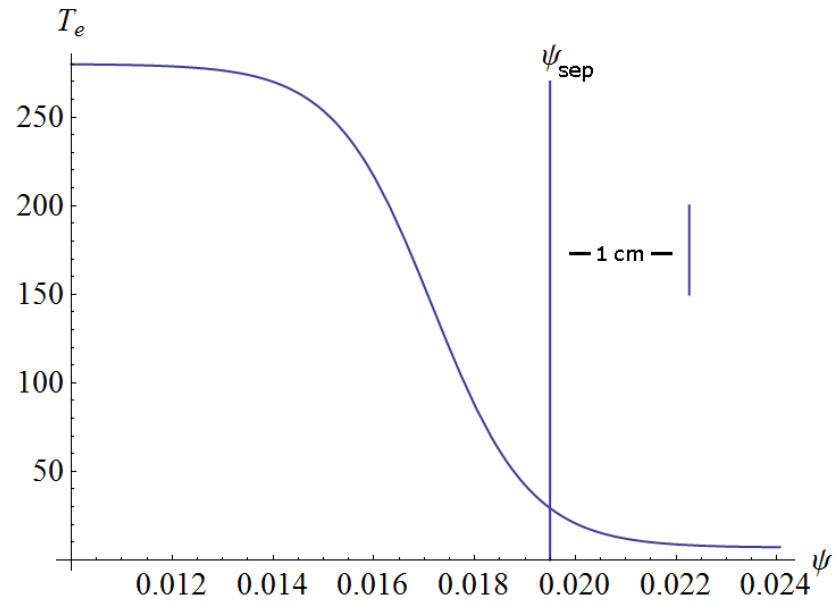

Test method

- Model equations:
  - Resistive ballooning mode.
  - Model contains curvature drive, electromagnetic $A_{||}$, collisional resistivity.
  - Conducting boundary conditions on divertor.

$$\gamma \nabla_\perp^2 \delta\phi = \frac{2\,B}{n} C_r\, \delta \mathrm{p} - \frac{B^2}{n} \partial_{\shortparallel} \nabla_\perp^2 \delta \mathrm{A}$$

$$\gamma \delta \mathrm{n} = -\delta \mathrm{v}_E \cdot \nabla n$$

$$-\gamma \nabla_\perp^2 \delta \mathrm{A} = \nu_e \nabla_\perp^2 \delta \mathrm{A} - \mu\, n \nabla_{\shortparallel} \delta\phi$$

where

$$C_r \equiv \vec{b} \times \kappa \cdot \nabla$$

$$\delta \mathrm{v}_E \cdot \nabla Q \equiv -i \frac{k_b (\partial_r Q)}{B} \delta\phi$$

$$\delta \vec{b} \cdot \nabla Q \equiv \frac{i\, k_b (\partial_r Q)}{\mu\, \delta_{\mathrm{er}}^2\, B} \delta \mathrm{A}$$

Results

- Robust instability at blob-relevant mode numbers in NSTX

Growth rate as a function of toroidal mode number for density at n = .79 x 10^{13} cm^{-3} (NSTX):

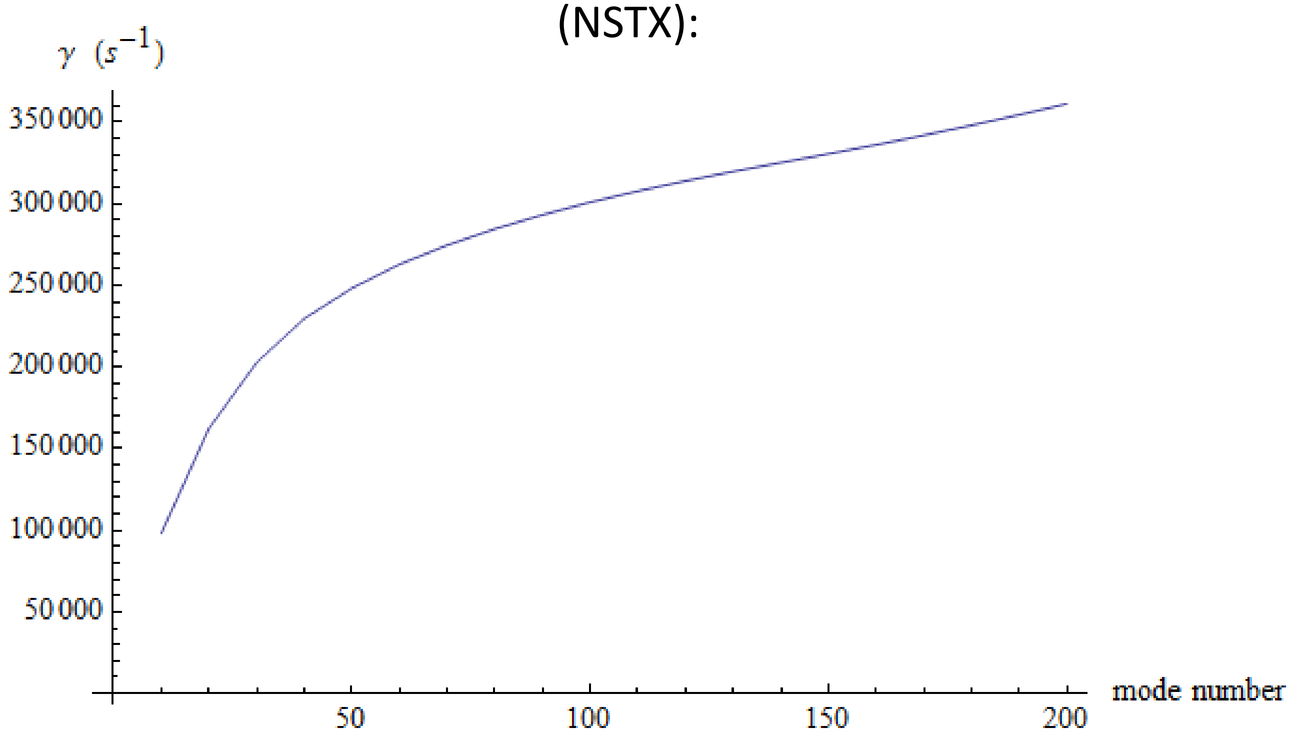

Results

- Collisionality impedes mode penetration to divertor in NSTX

Penetration ratio $\lambda/l_{X\text{-}D}{}^{*}$ as a function of temperature and density at mode peak for toroidal mode number 100 (NSTX):

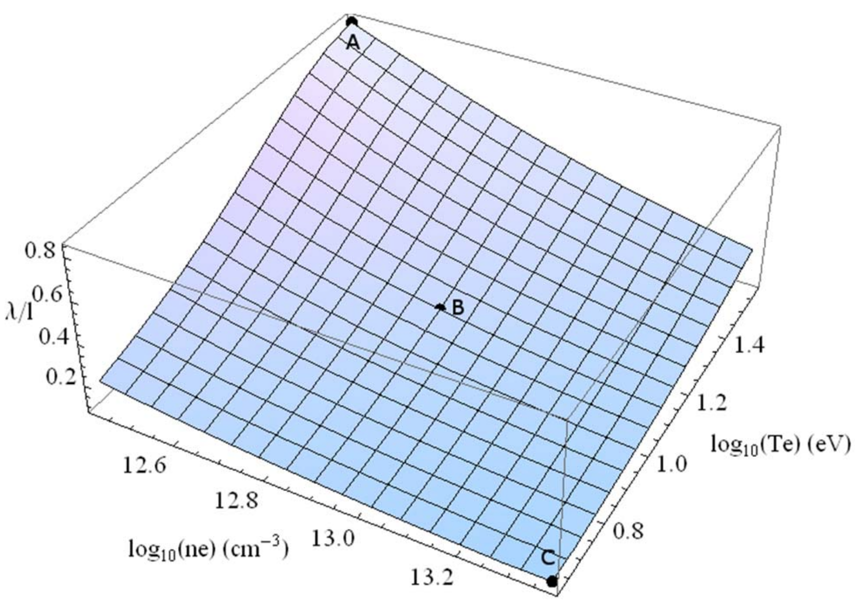

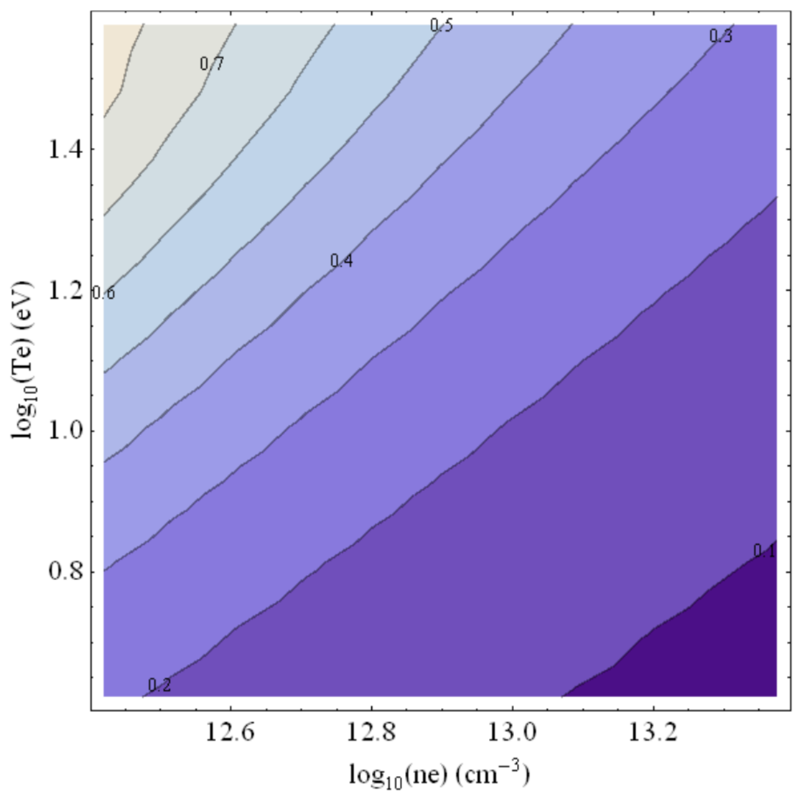

* $\lambda/l_{X\text{-}D}=-1/\mathrm{Ln}(\psi_{xpt}/\psi_{div})$

Lodestar

Results

- SOL modes do not reach divertor at high collisionality in NSTX

Spatial structure of eigenmode amplitude (ϕ) of fastest growing bump-localized mode for three test cases (NSTX):

A | B | C

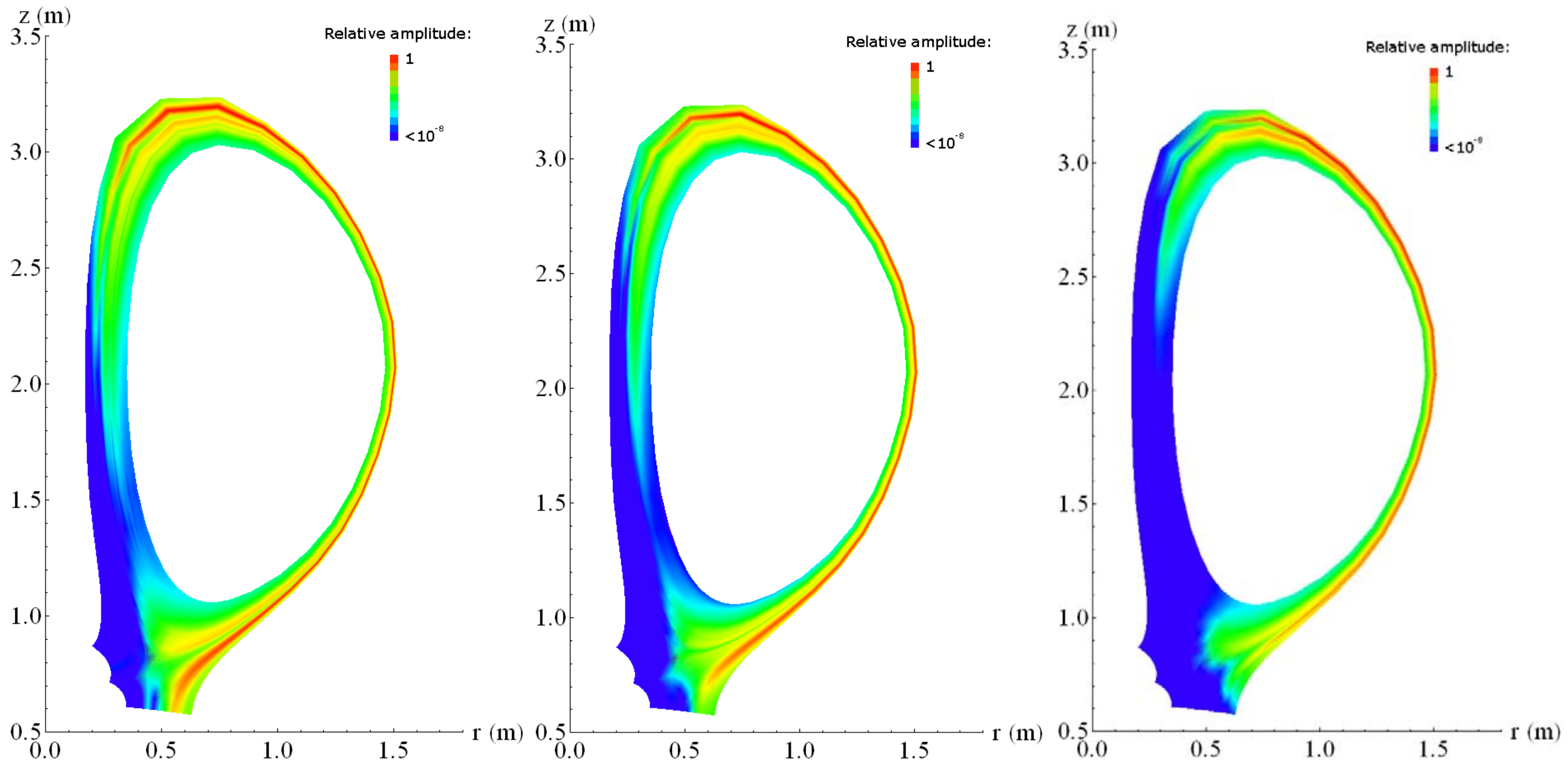

Bump n_e=2.63x10^{12}, T_e=37.8 eV | Bump n_e=7.9x10^{12}, T_e=12.6 eV | Bump n_e=2.37x10^{13}, T_e=4.2 eV

Results

- Robust instability at blob-relevant mode numbers in MAST

Growth rate as a function of toroidal mode number for density at bump peak of
$n = 5.31 \times 10^{12}\ cm^{-3}$ (MAST):

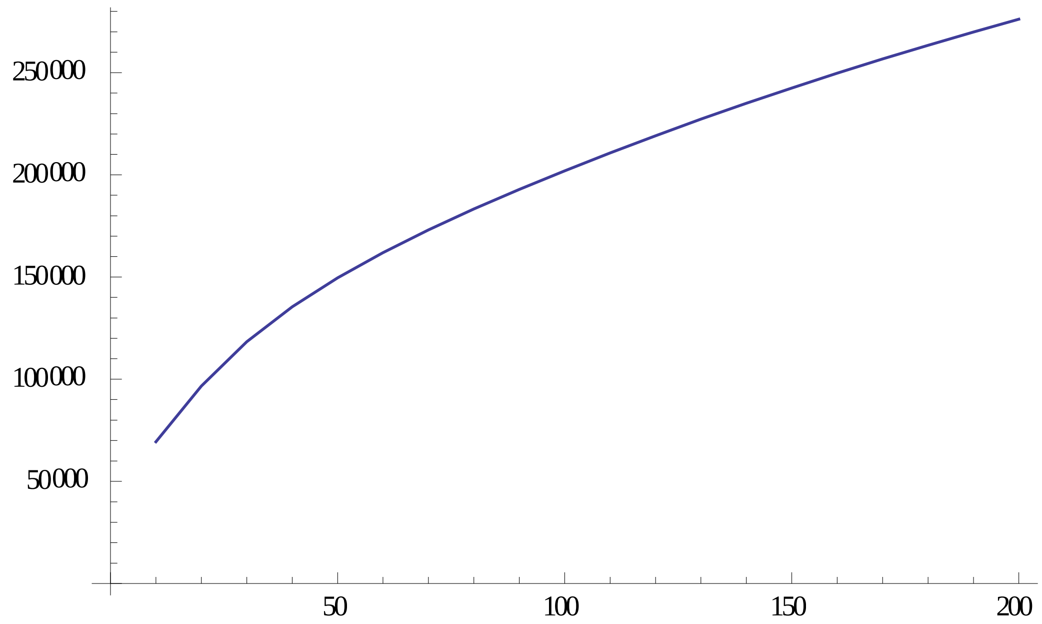

Results

- Collisionality impedes mode penetration to divertor in MAST

Penetration ratio $\lambda/l_{X\text{-}D}$ as a function of temperature and density at mode peak for toroidal mode number 100 (MAST):

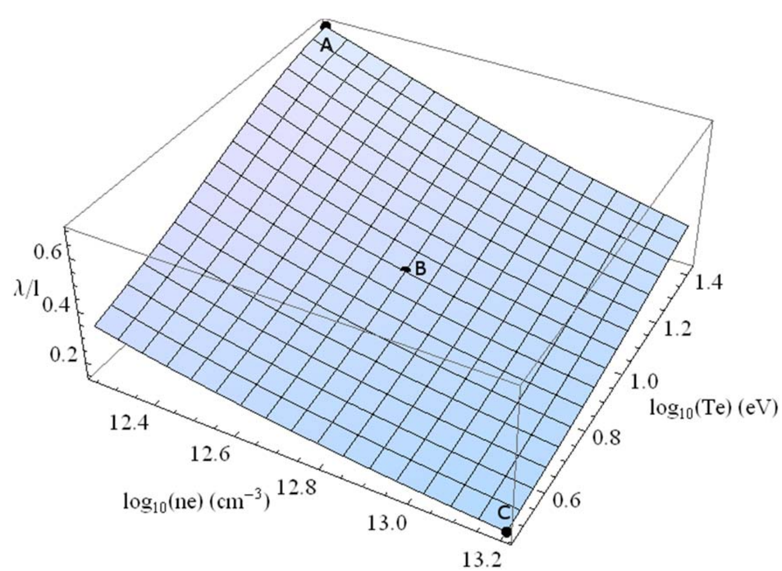

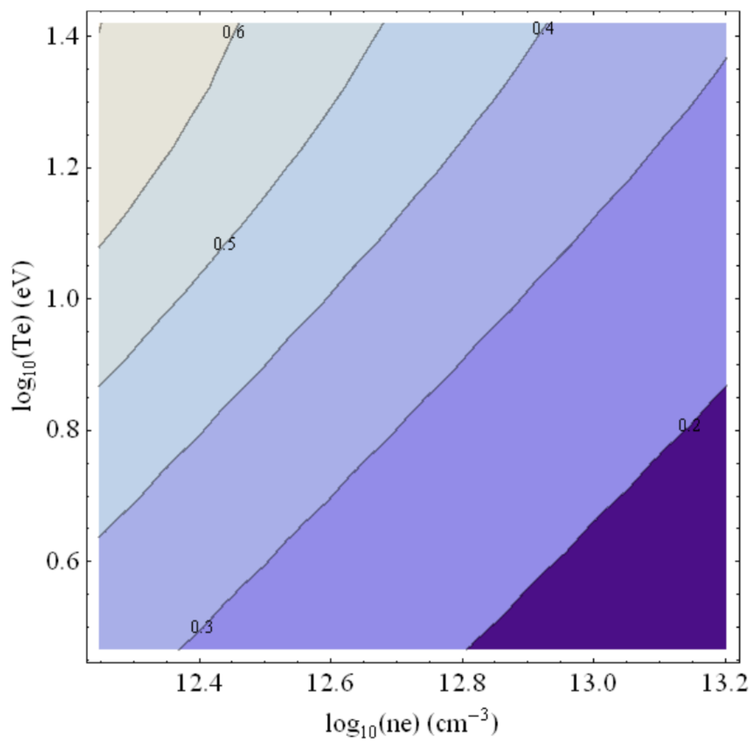

Results

- SOL modes do not reach divertor at moderate/high collisionality in MAST

Spatial structure of eigenmode amplitude (ϕ) of fastest growing bump-localized mode for three test cases (MAST):

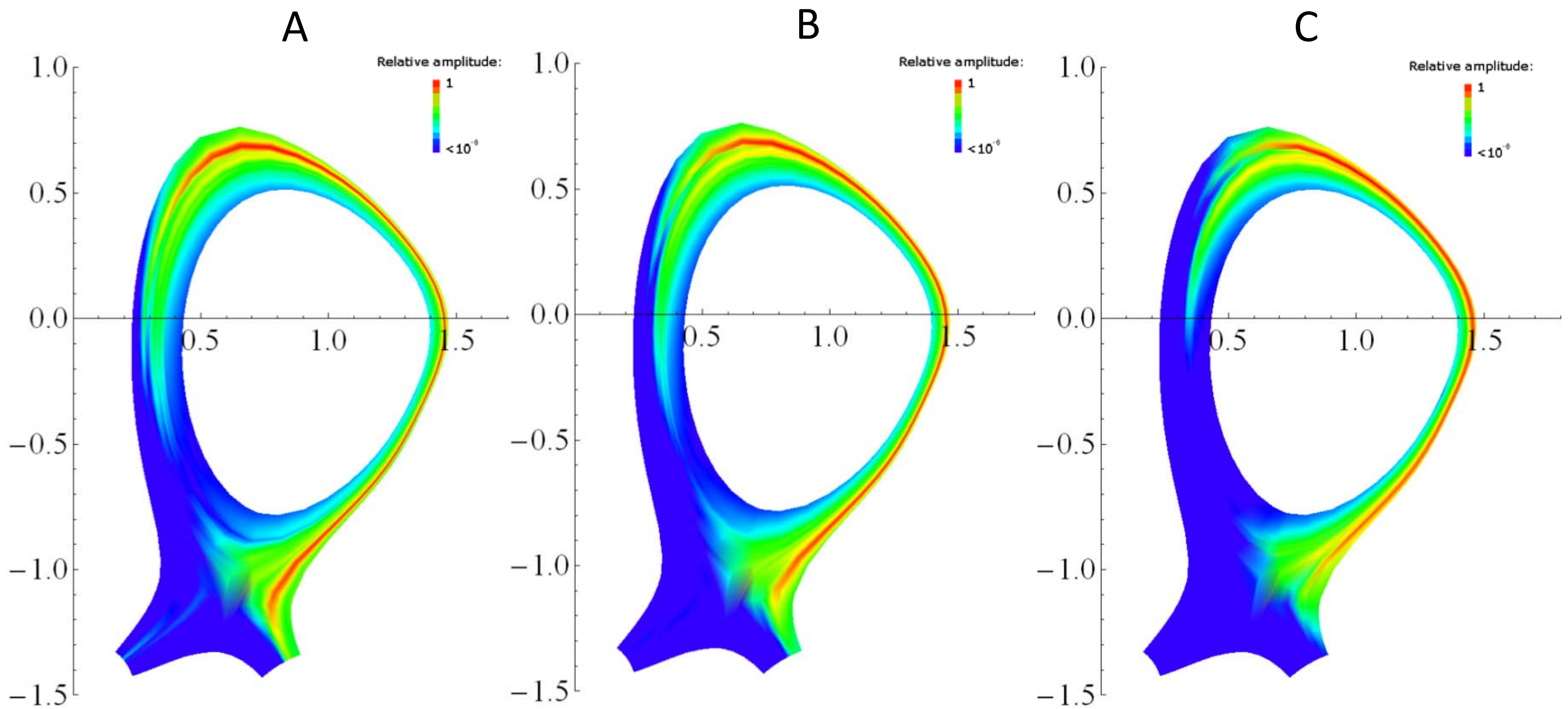

Bump n_e=1.77x10^{12}, T_e=2.92 eV   Bump n_e=5.31x10^{12}, T_e=8.77 eV   Bump n_e=1.59x10^{13}, T_e=26.3 eV

- Trends with temperature and density similar to those observed in NSTX.

Results

- Separatrix-localized mode fails to reach x-point in MAST
  - consistent with observed QXR

Spatial structure of eigenmode amplitude (ϕ) of fastest growing overall mode for three test cases (MAST):

A B C

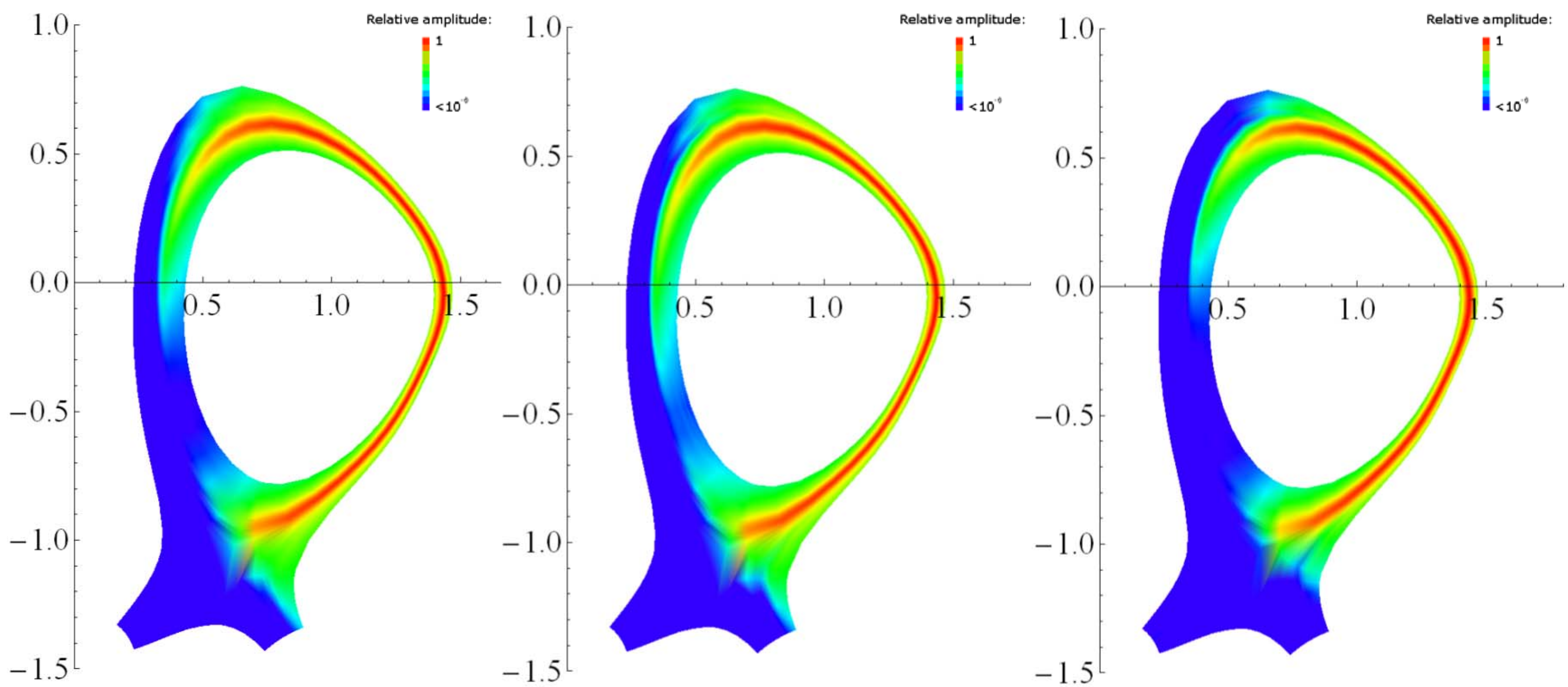

Bump n_e=1.77x10^{12}, T_e=2.92 eV   Bump n_e=5.31x10^{12}, T_e=8.77 eV   Bump n_e=1.59x10^{13}, T_e=26.3 eV

Results

- Self-consistent profile solver is being coupled to eigenmode filament solver

Growth rate as a function of temperature and density at mode peak using equilibrium solver for toroidal mode number 100 (NSTX):

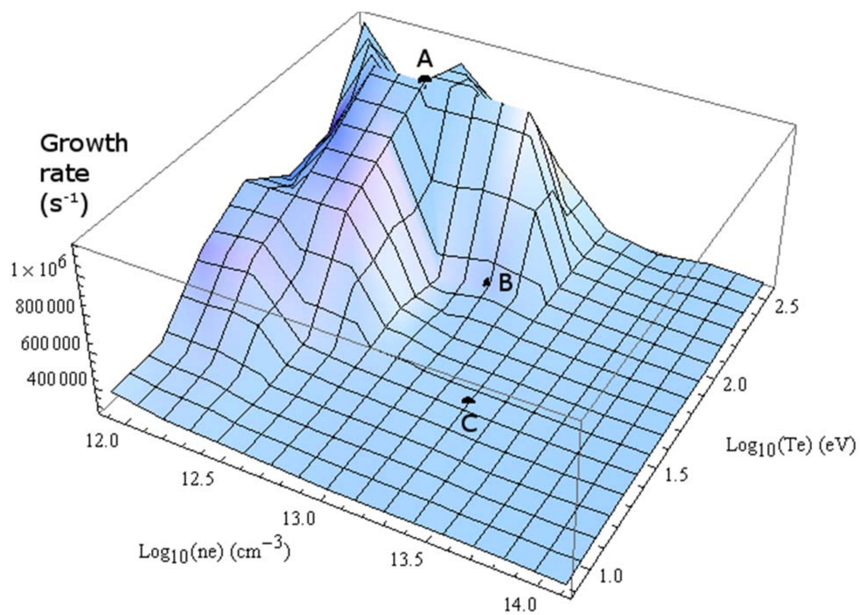

- Region of anomalous growth rates indicates multiple competing dominant eigenmodes.
- Change in dominant eigenmodes can be explained by changes in SOL width.
- Current version of equilibrium solver requires peak temperature and perpendicular conductivity as separate variables.
  - Makes maintaining a constant SOL width difficult to script.

Results

Spatial structure of eigenmode amplitude (ϕ)
for three test cases (NSTX) using equilibrium solver:

A

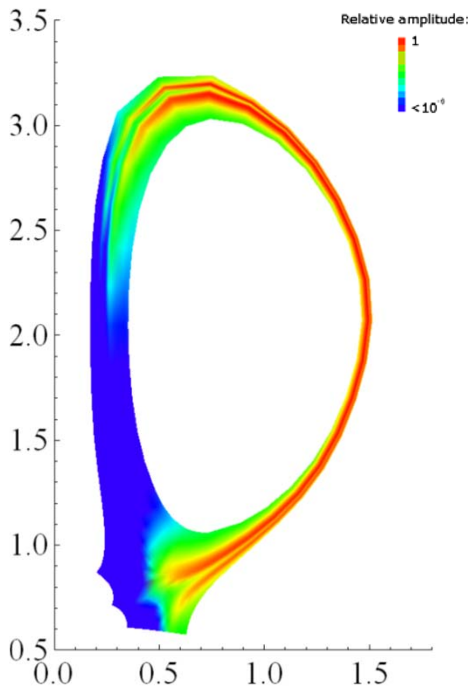

Peak n_e=1.73x10^{13},
T_e=526 eV

B

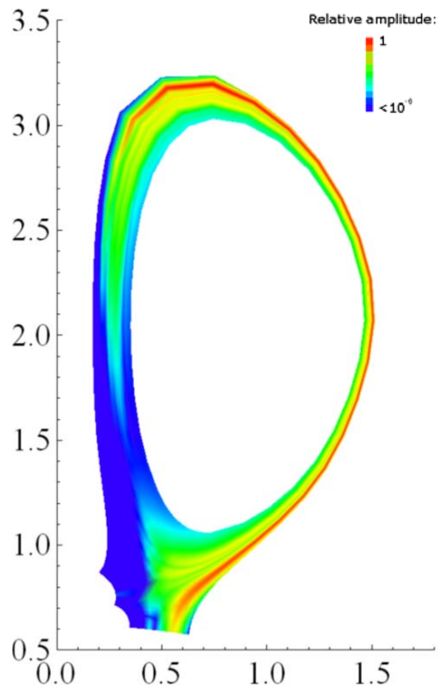

Peak n_e=2.99x10^{13},
T_e=399 eV

C

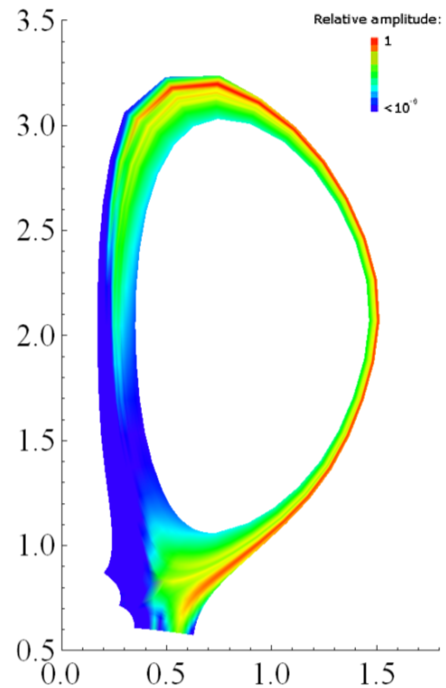

Peak n_e=3.94x10^{13},
T_e=231 eV

Results

Temperature profile for three test cases (NSTX) using equilibrium solver at χ_{perp}=2x10^{-9}:

A

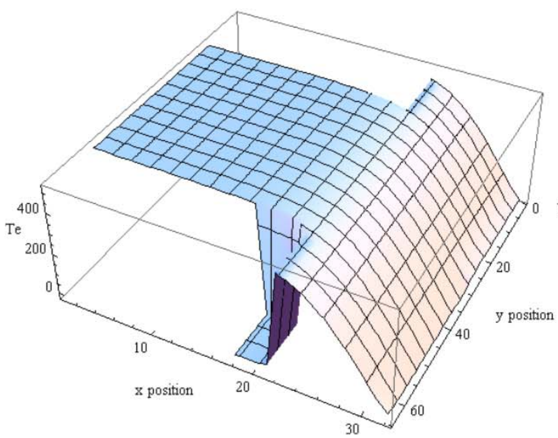

B

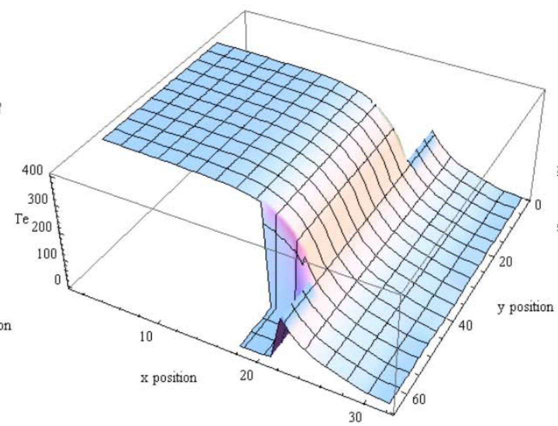

C

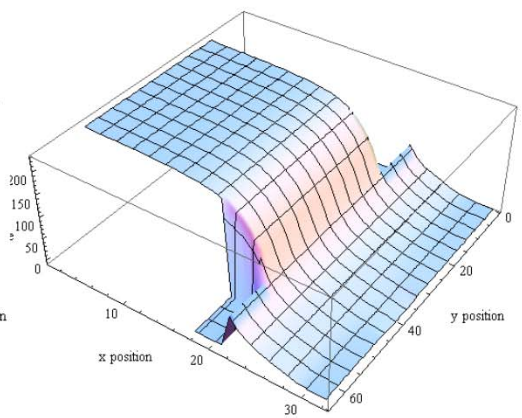

Peak n_e=1.73x10^{13},
T_e=526 eV

Peak n_e=2.99x10^{13},
T_e=399 eV

Peak n_e=3.94x10^{13},
T_e=231 eV

Conclusions

- Calculated filamentary structures compared in NSTX and MAST.
- Mode connection to divertor shows similar trends.
  - Increases with temperature.
  - Decreases with density.
- Strong variation in connection length with radial position.
  - Consistent with experimentally observed QXR in MAST.
- Work towards self-consistent profiles is in progress.
  - Self-consistent profile solver shows success in some test cases.
  - Not yet reliable enough for automated parameter scans.